

University of Groningen

Brown Carbon in Primary and Aged Coal Combustion Emission

Ni, Haiyan; Huang, Ru Jin; Pieber, Simone M.; Corbin, Joel C.; Stefenelli, Giulia; Pospisilova, Veronika; Klein, Felix; Gysel-Beer, Martin; Yang, Lu; Baltensperger, Urs

Published in:
Environmental Science and Technology

DOI:
[10.1021/acs.est.0c08084](https://doi.org/10.1021/acs.est.0c08084)

IMPORTANT NOTE: You are advised to consult the publisher's version (publisher's PDF) if you wish to cite from it. Please check the document version below.

Document Version
Publisher's PDF, also known as Version of record

Publication date:
2021

[Link to publication in University of Groningen/UMCG research database](#)

Citation for published version (APA):

Ni, H., Huang, R. J., Pieber, S. M., Corbin, J. C., Stefenelli, G., Pospisilova, V., Klein, F., Gysel-Beer, M., Yang, L., Baltensperger, U., Haddad, I. E., Slowik, J. G., Cao, J., Prévôt, A. S. H., & Dusek, U. (2021). Brown Carbon in Primary and Aged Coal Combustion Emission. *Environmental Science and Technology*, 55(9), 5701-5710. <https://doi.org/10.1021/acs.est.0c08084>

Copyright

Other than for strictly personal use, it is not permitted to download or to forward/distribute the text or part of it without the consent of the author(s) and/or copyright holder(s), unless the work is under an open content license (like Creative Commons).

The publication may also be distributed here under the terms of Article 25fa of the Dutch Copyright Act, indicated by the "Taverne" license. More information can be found on the University of Groningen website: <https://www.rug.nl/library/open-access/self-archiving-pure/taverne-amendment>.

Take-down policy

If you believe that this document breaches copyright please contact us providing details, and we will remove access to the work immediately and investigate your claim.

Downloaded from the University of Groningen/UMCG research database (Pure): <http://www.rug.nl/research/portal>. For technical reasons the number of authors shown on this cover page is limited to 10 maximum.

Brown Carbon in Primary and Aged Coal Combustion Emission

Haiyan Ni, Ru-Jin Huang,* Simone M. Pieber, Joel C. Corbin, Giulia Stafenelli, Veronika Pospisilova, Felix Klein, Martin Gysel-Beer, Lu Yang, Urs Baltensperger, Imad El Haddad, Jay G. Slowik, Junji Cao, André S. H. Prévôt, and Ulrike Dusek



Cite This: *Environ. Sci. Technol.* 2021, 55, 5701–5710



Read Online

ACCESS |



Metrics & More



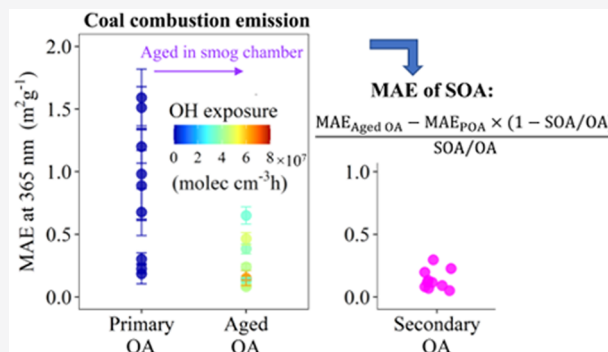
Article Recommendations



Supporting Information

ABSTRACT: Smog chamber experiments were conducted to characterize the light absorption of brown carbon (BrC) from primary and photochemically aged coal combustion emissions. Light absorption was measured by the UV–visible spectrophotometric analysis of water and methanol extracts of filter samples. The single-scattering albedo at 450 nm was 0.73 ± 0.10 for primary emissions and 0.75 ± 0.13 for aged emissions. The light absorption coefficient at 365 nm of methanol extracts was higher than that of water extracts by a factor of 10 for primary emissions and a factor of 7 for aged emissions. This suggests that the majority of BrC is water-insoluble even after aging. The mass absorption efficiency of this BrC (MAE_{365}) for primary OA (POA) was dependent on combustion conditions, with an average of $0.84 \pm 0.54 \text{ m}^2 \text{ g}^{-1}$, which was significantly higher than that for aged OA ($0.24 \pm 0.18 \text{ m}^2 \text{ g}^{-1}$). Secondary OA (SOA) dominated aged OA and the decreased MAE_{365} after aging indicates that SOA is less light absorbing than POA and/or that BrC is bleached (oxidized) with aging. The estimated MAE_{365} of SOA ($0.14 \pm 0.08 \text{ m}^2 \text{ g}^{-1}$) was much lower than that of POA. A comparison of MAE_{365} of residential coal combustion with other anthropogenic sources suggests that residential coal combustion emissions are among the strongest absorbing BrC organics.

KEYWORDS: light absorption efficiency, UV–vis spectrophotometric analysis, optical property, secondary organic aerosol, smog chamber



1. INTRODUCTION

Atmospheric aerosol affects the Earth's radiative balance by absorbing or scattering light and therefore warms or cools the atmosphere. Black carbon (BC) has been demonstrated to be one of the main light-absorbing components, while organic aerosol (OA) has long been thought to be a purely light-scattering component. However, a growing number of measurements have shown the existence of a fraction of OA with light-absorbing properties, referred to as brown carbon (BrC).^{1–3} BrC absorbs radiation mainly in the near UV and shorter visible wavelength range.^{4,5} The reported direct radiative effect of BrC varies significantly (e.g., from + 0.1 to + 0.6 W m^{-2}), and considerable uncertainties are associated with the still poor understanding of the optical properties and atmospheric evolution of BrC.^{6–11}

Atmospheric BrC has both primary and secondary sources. Primary BrC is emitted directly from biomass burning and fossil fuel combustion.^{12–16} The light absorption properties of primary BrC, however, vary considerably with combustion conditions and fuel types.^{16–18} Secondary BrC is formed in the atmosphere through oxidation and aging processes (Laskin et al.⁵ and references therein), which has been demonstrated in laboratory studies and often involves nitrogen-containing compounds.^{19,20} The light absorption of BrC can be further

modified through atmospheric processing. For example, the optical properties of BrC change with the hydroxyl radical (OH) exposure of the emissions. The formation and condensation of secondary OA (SOA) on the particles might add additional BrC. On the contrary, the chemical composition and optical properties of the existing BrC might be changed by, e.g., heterogeneous reactions in the aerosol phase, leading to bleaching.^{20–22}

Recent studies of BrC emissions have mainly focused on biomass burning,^{1,2,13,14,23,24} which produces a large amount of BrC relative to on-road vehicles.² A few studies have examined BrC from fossil fuel sources such as vehicles^{2,16} and coal combustion,^{25–27} focusing solely on primary emissions. Coal combustion is a particularly important pollution source of OA in China,^{28,29} India,³⁰ and some regions in Europe (e.g., Poland³¹ and Ireland³²). In China, coal consumption reached 4000 Tg in 2015, 93.5 Tg of which was combusted in

Received: November 30, 2020

Revised: March 1, 2021

Accepted: March 24, 2021

Published: April 7, 2021



residential sector.³³ A few very recent studies have found that coal combustion might also be an important source of BrC in China, especially during the heating season.^{34,35} However, our knowledge of BrC from coal combustion is still very limited, particularly with regard to its atmospheric evolution, which hinders the quantitative assessment of the climate effects of coal combustion OA and accurate modeling of aerosol radiative forcing. In this study, we present for the first time the light absorption properties of BrC from both primary and aged coal combustion emissions on the basis of controlled smog chamber experiments. This study discusses the effects of coal types, combustion conditions, and for the first time the effects of photochemical oxidation on the optical properties of BrC from coal combustion.

2. METHODS

2.1. Experimental Setup. Five coals were collected from major coal producing areas in China, including bituminous coals from Ningxia Province (B1), Inner Mongolia (B2), and Yunnan Province (B3) and anthracite coals from Shanxi Province (A1) and Shaanxi Province (A2; Table S1). The stove used (51 cm × 31 cm, height × diameter) is a typical Chinese coal burner and is described in Text S1 of the Supporting Information.

Figure S1 shows the experimental setup. Emissions were generated by burning batches of 200–300 g of coal in the stove (see Text S1 for the burning procedure). The stove was situated in a container connected to a chimney. Emissions were sampled from the chimney with a flow rate of about 1.5 L min⁻¹ through a heated (180 °C) silco steel line by either one or two ejector dilutors in series (Dekati Ltd.) to dilute the direct exhaust with zero air (737–250 series, AADCO Instruments, Inc.) and then injected into a precleaned Teflon smog chamber (7 m³; described in Text S2 and elsewhere^{36–38}), which provided an additional dilution. One ejector dilutor with a dilution ratio of 1:8–1:10 was used for anthracite coals, and two ejector dilutors in series (dilution ratios of 1:64 to 1:100) were used for bituminous coals, due to their considerable higher emissions than anthracite coals.

Emission injection into the chamber began from ignition and lasted for 30–50 min until coal fire emissions vanished. After the injection and stabilization of the primary emissions, nitrous acid (HONO)³⁹ was continuously injected into the chamber to provide OH radicals through irradiation. Then, 1 μL of deuterated butanol-D9 (98%, Cambridge Isotope Laboratories) was injected to monitor the OH exposure.⁴⁰ Emissions were aged with UV lights for 4–6 h. Aging is equivalent to 0.5–1.7 days of OH-driven photochemistry under atmospheric concentrations (OH = 2 × 10⁶ molecules cm⁻³). Control experiments (i.e., experiments performed analogous to the emission aging but without injecting emissions in the smog chamber) were conducted regularly to estimate the background. For each burning experiment and control experiment, primary and aged particles from the smog chamber were collected on quartz fiber filters (47 mm diameter, Pall Corporation; 20 L min⁻¹) for 20–30 min for offline UV–visible measurements (Table S2). A charcoal denuder was installed upstream of the filter sampler to remove organic gases. The collected filters were immediately stored at –20 °C until analysis.

A set of online instruments was connected to the smog chamber to characterize the particle phase before and after UV lights on. The concentration of butanol-D9 was monitored by

a proton transfer reaction time-of-flight mass spectrometer (PTR-TOF-MS, Ionicon Analytik).⁴¹ The decay of butanol-D9 was used to infer the time-integrated OH.⁴⁰ A high-resolution time-of-flight aerosol mass spectrometer (HR-ToF-AMS, Aerodyne Research Inc.) equipped with a PM_{2.5} aerodynamic lens⁴² was used to measure the nonrefractory particle phase composition.⁴³ A collection efficiency of 1 was applied to the HR-ToF-AMS data. Equivalent black carbon (eBC) measurements (Text S3) were conducted with an Aethalometer (Model AE33, Magee Scientific).⁴⁴ Single-scattering albedo (SSA) measurements were obtained with three CAPS PM_{SSA} monitors operating at 450, 630, and 780 nm (Aerodyne Research Inc.). The three instruments reported similar trends in SSA. Figure S2 illustrates the dynamic change of eBC and OA concentrations for experiment B1-03 of coal B1. Before lights on, the eBC and OA concentrations decreased due to wall loss. The primary particles offered a sufficiently large condensation sink. When the lights were turned on and the primary coal combustion exhaust was exposed to atmospheric oxidants, the SOA formed via oxidation of precursor gases and condensed on existing particles.^{45,46} A rapid increase in OA concentrations from SOA formation was observed due to the SOA production rate exceeding the wall loss. From the third hour, the increase rate of OA concentrations slowed down as the SOA production rate became smaller and the wall loss rate started to dominate.

2.2. Off-Line UV–Visible Measurements and Light Absorption Characterization. Water and methanol extracts of each filter sample were prepared for the UV–vis measurements (Text S4). The light absorption spectra of the liquid extracts were measured over the wavelength range 280–500 nm using a UV–visible spectrophotometer (Ocean Optics) coupled to a 50 cm long-path detection cell.^{3,23,47} The recorded wavelength-dependent attenuation was corrected for background signal and was converted to the absorption coefficient of the diluted solution at a given wavelength λ ($b_{\text{abs},\lambda}$ in Mm⁻¹; eq S1). The $b_{\text{abs},\lambda}$ of aging blanks collected during control experiments was comparable to that of blank filters collected from the cleaned chamber. Therefore, the $b_{\text{abs},\lambda}$ values of the blanks were averaged and subtracted from the $b_{\text{abs},\lambda}$ values of both primary and aged aerosol for blank correction (Figures S3 and S4).

From $b_{\text{abs},\lambda}$, the mass absorption efficiency of the solubilized OA fraction (MAE in m² g⁻¹) can be quantified as eq 1. Here, the solution MAE is different from the widely known term “mass absorption cross section (MAC)”, which refers to particles in the air.

$$\text{MAE}_\lambda = \frac{b_{\text{abs},\lambda}}{C_{\text{OA}}} \quad (1)$$

where C_{OA} is the mass concentration of extracted organics ($\mu\text{g m}^{-3}$) and can be expressed as

$$C_{\text{OA}} = \frac{\text{EE} \times M_{\text{OA}}}{V_{\text{air}}} \quad (2)$$

where EE denotes the OA extraction efficiency and M_{OA} is the total OA mass on the filter. M_{OA} was calculated by an integration of the OA mass concentrations measured by the AMS times the filter sampling flow rate over the corresponding sampling period of the filter (Table S3). EE could not be measured directly. On the basis of previous work,^{1,48} we assumed an EE for methanol of unity in the following

discussion. Since $b_{\text{abs},\lambda}$ was determined from the particles collected on the filters and C_{OA} was measured online during the filter collection time, no wall loss correction was applied to either $b_{\text{abs},\lambda}$ or C_{OA} for consistency. If particles with different sizes have both different MAE and different wall loss rates, this could lead to changes in MAE with time that are not related to emission aging. However, this should have limited influence on the MAE, as a very recent study showed that particle size distribution and light absorption did not change due to particle wall loss in a similar chamber experiment.⁴⁹

The solution absorption Ångström exponent (AAE, where $b_{\text{abs},\lambda} \propto \lambda^{-\text{AAE}}$) is a measure of the absorption wavelength dependence and is determined by applying a linear regression fit to the logarithms of $b_{\text{abs},\lambda}$ and wavelength. The applicable range of the fit (300–500 nm for methanol extracts and 300–400 nm for water extracts) was determined by the linear region of $b_{\text{abs},\lambda}$ and wavelength on log–log plots.

2.3. Determination of b_{abs} and MAE of SOA. The aged OA in this study includes both POA and SOA, thus b_{abs} of SOA ($b_{\text{abs,SOA}}$) can be calculated from b_{abs} of aged OA and POA in the aged aerosol:

$$b_{\text{abs,SOA}}(t) = b_{\text{abs,aged OA}}(t) - b_{\text{abs,POA}}(t) \quad (3)$$

where t is the time period during which the filters of the aged aerosol were collected. $b_{\text{abs,aged OA}}(t)$ was directly measured with uncertainties derived from eq S3 in Text S5; $b_{\text{abs,POA}}(t)$ can be estimated by

$$b_{\text{abs,POA}}(t) = \text{MAE}_{\text{POA}} \times \text{POA}(t) \quad (4)$$

POA(t) can be inferred from the initial OA mass concentrations in the primary emissions, assuming that the POA and BC are lost to the walls at an equal rate:

$$\text{POA}(t) = \text{OA}(t_0) \times \exp\left(\frac{-(t - t_0)}{\tau}\right) \quad (5)$$

where OA(t_0) is the mass concentration of OA measured by the AMS at t_0 before aging. τ is the wall loss constant, determined using a fitted eBC concentration. Two different fits were used, one before lights on when no change in light absorption from particle coating is expected ($\tau = 2.6 \pm 0.4$) and the other at the end of the experiment when particle growth is negligible ($\tau = 3.7 \pm 1.0$). The average of τ from the two fits was chosen as the best estimate.

The MAE and mass of SOA in the aged emissions can be formulated as

$$\text{MAE}_{\text{SOA}}(t) = \frac{\text{MAE}_{\text{aged OA}}(t) - \text{MAE}_{\text{POA}} \times (1 - \text{SOA}(t)/\text{OA}(t))}{\text{SOA}(t)/\text{OA}(t)} \quad (6)$$

$$\text{SOA}(t) = \text{OA}(t) - \text{POA}(t) \quad (7)$$

The MAE_{POA} is assumed to be constant during the aging experiment, meaning that the effect of photochemical aging on the light absorption of POA is neglected. However, it is possible that a chemical transformation of POA occurs, resulting in an altered mass and/or MAE of POA during aging. If any changes of MAE_{POA} occur, this results in a changed estimate of the MAE_{SOA} . The sensitivity of MAE_{SOA} to hypothetical changes in MAE_{POA} by POA aging is shown in the Figure S5 and is small, except for experiments B3-10 and B3-12. Due to the small contribution of POA to the aged OA, the $\text{SOA}(t)/\text{OA}(t)$ and MAE_{SOA} are not sensitive to a possible

decrease in POA mass due to aging (Text S6 and Figure S6). In general, moderate changes in mass and MAE of POA during aging will not affect our conclusion that MAE_{SOA} is much smaller than MAE_{POA} . Uncertainties of MAE_{SOA} and $\text{SOA}(t)$ were propagated from $\text{OA}(t_0)$, $\text{OA}(t)$, $\text{MAE}_{\text{aged OA}}$ and MAE_{POA} through eqs 5–7.

3. RESULTS AND DISCUSSION

3.1. Differences between the b_{abs} of Water and Methanol Extracts.

Figure 1 compares b_{abs} of methanol and

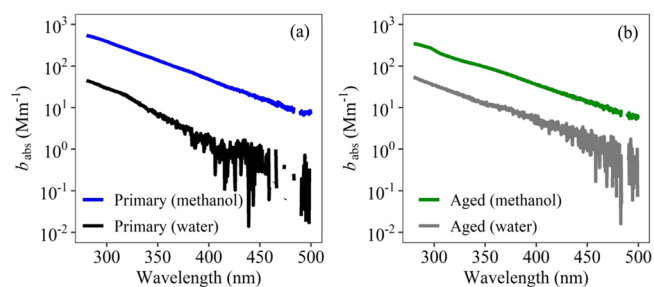


Figure 1. Example solution spectra of methanol and water extracts from the primary and aged samples of bituminous coal B1 (experiment B1-01). All the b_{abs} values (Mm^{-1}) are corrected for blanks (Figure S3) but are not wall loss corrected.

water extracts from the primary and aged emissions of experiment B1-01 (coal B1, Table S2), as a typical example for emissions from bituminous coal. Note that for anthracite coals (coal A1 and A2) the b_{abs} of BrC from both primary and aged emissions was below or very close to the blank signal (Figure S3), thus the samples from the anthracite coals are excluded in the discussion below. Anthracite coal is much cleaner than bituminous coal, as observed in our companion work on both gas- and particle-phase emissions.^{41,50} Light absorption of the water and methanol extracts for both primary and aged BrC shows a characteristic wavelength dependence, decreasing with increasing wavelength from the ultraviolet to visible range.^{1,2,51,52} The absorption of the methanol extracts decreases more slowly with wavelength compared to that of water extracts, leading to a lower AAE of the methanol extracts than of the water extracts (Figure 1). This is consistent with previous studies for both ambient observations^{48,53,54} and source emissions^{1,16} and could be attributed to the presence of higher molecular weight chromophores, which are exclusively dissolved in methanol and absorb light at longer wavelengths.^{1,53,54}

For the same (primary or aged) filter samples, the b_{abs} of the methanol extract is always larger than that of the water extract over the wavelength range 280–500 nm, because both water-soluble and water-insoluble organic compounds can be extracted by methanol.^{1,35,48} For all the bituminous coals (coal B1, B2, and B3), the b_{abs} at 365 nm of the methanol extracts was on average 10 and 7 times higher than that of the water extracts for primary and aged emissions, respectively. This suggests that OC extractable by methanol provides a better estimation of the total BrC compared to water-soluble organics. Due to the low light absorbance of water extracts, for some samples, data were very noisy (i.e., a low signal-to-noise ratio) at the wavelength >400 nm. Furthermore, for the water extracts, the b_{abs} of some coal samples was very close to that of the blank filters, leading to large uncertainties in b_{abs} after blank

correction. Therefore, only the optical properties of methanol-extracted BrC are discussed in the following sections.

3.2. MAE of Primary and Aged Emissions. 3.2.1. MAE of Primary Emissions. Figure 2 shows the MAE (i.e., inferred

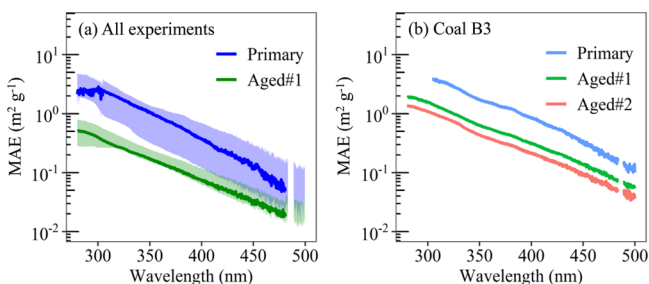


Figure 2. MAE of primary and aged OA extracted in methanol for (a) all experiments including all bituminous coals (coal B1, B2, and B3) and (b) coal B3. In panel a, the bold line indicates the median and the shaded areas indicate the interquartile range (25th–75th percentiles) of the median. During each experiment, at least one aged sample (aged#1) was collected after the UV lights were turned on. For coal B3, another aged sample (aged#2) was collected at the end of the aging experiment (OH exposure: aged#2 > aged#1, see Table S3).

from the b_{abs} and the $C_{\text{OA}i}$ eq 1) of the methanol extracts as a function of wavelength. The MAE_{365} (i.e., MAE averaged between 360 and 370 nm) was used as a proxy of the concentration of organic chromophore components (or BrC).⁵ Considerable variability in MAE_{365} of POA ($\text{MAE}_{\text{POA},365}$) was observed for different types of coal and for different experiments of the same type of coal.

Figure 3a shows that the $\text{MAE}_{\text{POA},365}$ of methanol extracts increased with a decreasing f_{OA} mass ratio (i.e., OA/(OA+eBC) ($r^2 = 0.84$)). Therefore, the MAE_{365} of primary BrC from

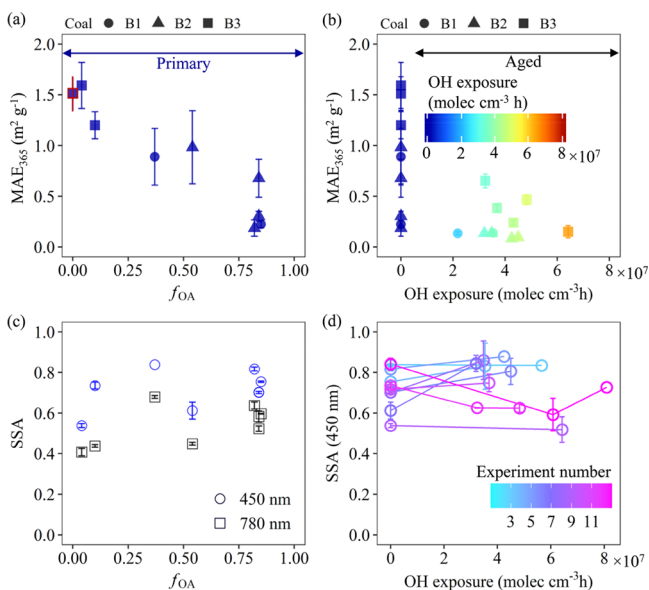


Figure 3. MAE at 365 nm of methanol extracts and single-scattering albedo (SSA) (a and c) as a function of f_{OA} for primary emissions and (b and d) as a function of OH exposure for both primary (OH exposure = 0) and aged emissions. In panel a, experiment B3-10 is plotted on $f_{\text{OA}} = 0$, because its f_{OA} is not available due to instrument failure of eBC measurements using the Aethalometer. The uncertainties of MAE and SSA are shown as vertical bars (Text S5). See Table S3 for experiment numbers.

coal combustion is dependent on combustion conditions, which is largely indicated by f_{OA} .¹⁶ The f_{OA} for smoldering combustion was demonstrated to be higher than that for flaming combustion,^{55,56} because flaming high-temperature combustion favors the formation and emission of BC and the smoldering combustion produces more incomplete combustion products, resulting in higher OA than BC (thus a higher f_{OA}). Figure 3a shows very different f_{OA} values, even for the combustion of the same coal, although we took care to minimize variability in parameters influencing the combustion conditions (e.g., the fuel mass, the size of the coal pieces, and the temperature of the smoldering coals used to ignite the sample; Table S2). This variability was not correlated with the duration of the preflaming combustion phase, which is defined as the time from introducing the sample coal to the preheated stove until the flaming fire begins. The longest preflaming phase was three times longer than the shortest. We consider that variability in the nature (structure and composition) of the different coal samples was the cause of the observed variability in f_{OA} . Compared to coal B1 and B2, the f_{OA} for coal B3 was lower (i.e., high BC and low OA fractions), indicating different chemical compositions of particle emissions. This is similar to our finding for the composition of gas-phase organics that coal B3 emits more aromatic compounds ($\sim 50\%$) but much less oxygenated aromatic compounds (10%) than B1 and B2.⁴¹

The averaged $\text{MAE}_{\text{POA},365}$ was $1.43 \pm 0.21 \text{ m}^2 \text{ g}^{-1}$ for coal B3, $0.54 \pm 0.36 \text{ m}^2 \text{ g}^{-1}$ for B2, and $0.56 \text{ m}^2 \text{ g}^{-1}$ for B1 (Table S4). The higher $\text{MAE}_{\text{POA},365}$ for coal B3 can be expected from its much lower f_{OA} than those of B1 and B2 (Figure 3a). A lower f_{OA} indicates more BC relative to OA, and more BC is generally associated with high-temperature flaming combustion. Previous studies found that a high temperature leads to carbonization rather than pyrolysis of the fuel, resulting in a reduced emission of volatile carbon compounds and a larger MAE.^{1,57} On the basis of Mie modeling, Saleh et al.¹⁸ also proposed that combustion conditions leading to higher BC fractions, hence lower f_{OA} , are favorable for the formation of large organic compounds that are highly light absorbing. This trend was also directly observed for methanol extracts of wood-burning OA by Kumar et al.²³

3.2.2. Differences in MAE between Primary and Aged Aerosols. The optical properties of OA from coal combustion can evolve during aging in the atmosphere. After 4–6 h aging, the OA concentrations increased 1.4–11 times (without wall losses correction) due to SOA formation (Table S3). The MAE of methanol extracts from aged OA ($\text{MAE}_{\text{aged OA}}$) was lower than the MAE_{POA} over the wavelength range 280–500 nm (Figure 2). Figure 3b shows MAE_{365} as a function of OH exposure (aging). MAE_{365} decreased from 0.56 to $0.14 \text{ m}^2 \text{ g}^{-1}$ for coal B1, from 0.54 ± 0.36 to $0.11 \pm 0.03 \text{ m}^2 \text{ g}^{-1}$ for B2, and from 1.43 ± 0.21 to $0.38 \pm 0.20 \text{ m}^2 \text{ g}^{-1}$ for B3, from primary to aged aerosols. The decreased MAE with aging suggests either the production of SOA, which is less light absorbing than the POA, or the conversion of POA to a less absorbing material during aging (“bleaching”, e.g., chemical reactions resulting in the destruction of the chromophores). The decreasing trend of light absorption in aged coal emissions is consistent with previous results of laboratory experiments^{18,20,22–24} and field observations^{10,21,58} on emissions from biomass burning or laboratory proxies of atmospheric BrC.

The SSA of the primary aerosol at 450 and 780 nm did not show a strong dependence on f_{OA} (Figure 3c). In all experiments, the SSA at 450 nm for primary emissions was

0.73 ± 0.10 . The SSA did not change significantly due to aging (SSA at 450 nm of aged emissions was 0.75 ± 0.13 ; Figure 3d) and was low enough for this aerosol to result in a positive forcing on average (e.g., < 0.85).^{59,60}

3.2.3. Wavelength Dependence of MAE. The AAE of methanol extracts averaged to 7.2 ± 1.25 for primary emissions (Figure 4). Different coal types showed different primary AAE

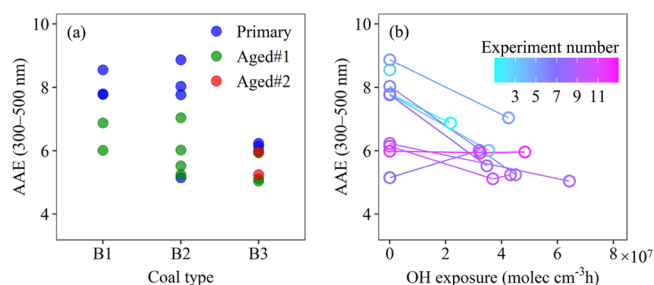


Figure 4. Absorption Ångström exponent (AAE; determined from the wavelength range 300–500 nm) of methanol-soluble BrC, varying by (a) coal type and (b) OH exposure (aging) for different experiments. See Table S3 for experiment numbers.

values. For primary emissions, the AAE of coal B3 (6.1 ± 0.44) was smaller than those of B1 (8.0 ± 1.6) and B2 (7.5 ± 0.12). This could be explained by the lower f_{OA} of B3 (Table S3), which, to a large extent, is an indicator of combustion conditions. Earlier studies found that a lower f_{OA} is associated with a lower AAE.^{17,18,23} Our AAE values are consistent with those reported in Yan et al.³⁵ and Li et al.,²⁵ the only two studies available that reported methanol-extracted AAE values

(7.46 ± 0.77 and $7.7\text{--}12$, respectively) from primary coal combustion emissions.

The AAE of methanol extracts from primary emissions was variable for different coal types (Figure 4a), but it converges to a much narrower range after aging (Figure 4b). In general, the AAE of methanol extracts from aerosol samples after aging was lower than that from primary emissions, averaging 6.4 for coal B1, 5.9 ± 0.8 for B2, and 5.5 ± 0.4 for B3, respectively. This suggests that SOA formation might change the light-absorbing ability of particles (Laskin et al.⁵ and references therein).

3.3. MAE of SOA. The mass, b_{abs} , and MAE of SOA in aged OA were estimated according to eqs 3–7, as detailed in Section 2.3. SOA dominated the aged OA mass, with $\text{SOA}(t)/\text{OA}(t)$ ranging from 0.61 to 0.98 with an average of 0.88 during the time period t when the aged aerosols were collected (Figure 5a). An increase in $\text{SOA}(t)/\text{OA}(t)$ with increasing aging time and OH exposure was observed for experiments B3-10, B3-12, and B3-13, during which two filters (i.e., referred to as aged OA#1 and aged OA#2; Table S3) were collected at different times after lights on. This shows continuing SOA formation with longer aging times. Both SOA and POA contributed to the overall $b_{\text{abs,aged OA}}$, with SOA accounting for $58 \pm 26\%$ of $b_{\text{abs,aged OA}}$ at 365 nm observed at the chamber (Figure 5b). The averaged contribution of $b_{\text{abs,SOA}}$ to $b_{\text{abs,aged OA}}$ was higher for coal B1 and B2 ($82 \pm 6\%$) than for coal B3 ($34 \pm 7\%$), due to a higher MAE_{POA} and a lower-than-average $\text{SOA}(t)/\text{OA}(t)$ for coal B3. These SOA contributions to the overall $b_{\text{abs,aged OA}}$ are at higher estimates, because more POA is lost to the wall than SOA, which only forms later in the experiments.

Figure 5c shows the MAE_{SOA} and $\text{MAE}_{\text{aged OA}}$ at 365 nm. For coal B1 and B2, the estimated $\text{MAE}_{\text{SOA,365}}$ values ($0.10 \pm$

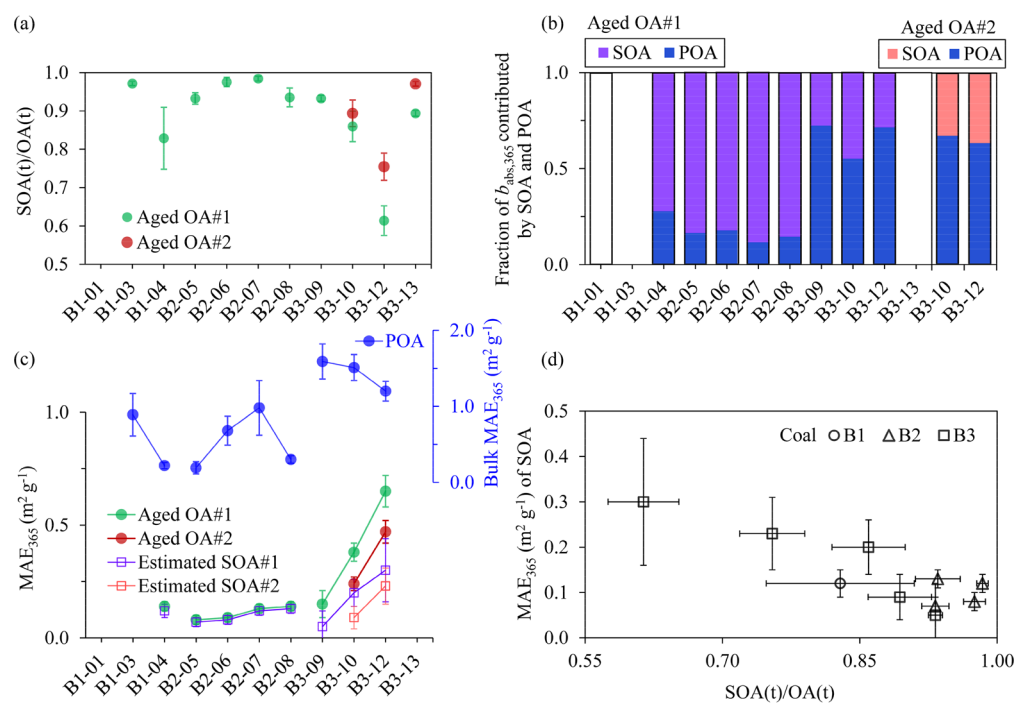


Figure 5. (a) Proportion of SOA in the aged OA ($\text{SOA}(t)/\text{OA}(t)$) during the time period t when the aged aerosols were collected. For experiments B3-10, B3-12, and B3-13, two filters (i.e., aged OA#1 and aged OA#2) were collected after UV light on (aging starts). (b) Fraction of $b_{\text{abs,365}}$ of aged OA (total bar heights) contributed by SOA and POA. The b_{abs} values for POA and SOA in aged OA are indicated using different color bars. (c) MAE at 365 nm for measured POA, aged OA, and estimated SOA. (d) MAE at 365 nm of SOA as a function of $\text{SOA}(t)/\text{OA}(t)$.

Table 1. MAE at 365 nm (MAE_{365}) of Primary Emissions from Different Sources Measured by UV–Vis Spectrometry

emissions sources	fuels/subtypes	regions	solvent	extraction efficiency ^a	$MAE_{365}(\text{m}^2 \text{g}^{-1})$ [i.e., normalizing b_{abs} to] ^f	$MAE_{365}(\text{m}^2 \text{g}^{-1} \text{C})$ [i.e., normalizing b_{abs} to] ^f	references
residential coal combustion	all coals	China	water		NA ^b	NA ^b	this study
	anthracite coal, A1 and A2	China	methanol		NA ^b	NA ^b	this study
	bituminous coal, B1	China	methanol		0.56 (0.22–0.89) [OA ^c]	0.83 (0.33–1.34) [OC ^d]	this study
	bituminous coal, B2	China	methanol		0.54 ± 0.36 (0.20–0.98) [OA]	0.81 ± 0.54 (0.30–1.47) [OC]	this study
	bituminous coal, B3	China	methanol		1.43 ± 0.21 (1.20–1.59) [OA]	2.15 ± 0.31 (1.80–2.39) [OC]	this study
			China	water	13 ± 10% of OC	1.10 ± 0.16 [WSOC] ^e	1.57 ± 0.78 [WIOC] ^e
vehicular emissions	bituminous coal	China	methanol	100% of OC ^e		1.51 [OC]	Yan et al. ³⁵
		China	water	4.3–16% of TC		0.3–0.7 [WSOC]	Li et al. ²⁵
		China	methanol	93–98% of TC		1.2–2.8 [MSOC]	Li et al. ²⁵
	anthracite coal	China	water	24–46% of TC		0.9–1.0 [WSOC]	Li et al. ²⁵
		China	methanol	76–98% of TC		0.9–2.4 [MSOC]	Li et al. ²⁵
	bituminous coal	China	water	23–38% of OC		0.1–1.0 [WSOC]	Wang et al. ⁶²
		China	methanol	81–84% of OC		0.7–1.7 [MSOC]	Wang et al. ⁶²
	tractor	China	water			1.33 ± 0.49 [WSOC]	Du et al. ⁶³
	motorcycle	China	water			0.20 ± 0.08 [WSOC]	Du et al. ⁶³
	gasoline + diesel vehicles	China	water			0.71 ± 0.17 [WSOC]	Hu et al. ⁶⁴
biomass burning	gasoline vehicles	U. S.	methanol	75.9 ± 9.42% of OC		0.62 ± 0.76 [OC]	Xie et al. ¹⁶
	wood	China	water			0.97 ± 0.26 [WSOC]	Du et al. ⁶³
	grass	China	water			0.90 ± 0.07 [WSOC]	Du et al. ⁶³
	corn	China	water			1.05 ± 0.08 [WSOC]	Du et al. ⁶³
	yak dung + wood	China	water			0.91 ± 0.18 [WSOC]	Hu et al. ⁶⁴
	Kentucky blue grass residues	U. S.	methanol	94.5 ± 2.01% of OC		1.80 ± 0.15 [OC]	Xie et al. ¹⁶
	wheat stubble	U. S.	methanol	94.5 ± 2.97% of OC		1.28 ± 0.12 [OC]	Xie et al. ¹⁶
	wheat + herbicide	U. S.	methanol	91.5 ± 3.17% of OC		2.09 ± 0.12 [OC]	Xie et al. ¹⁶
	forest bum	U. S.	methanol	97 ± 1.87% of OC		1.13 ± 0.15 [OC]	Xie et al. ¹⁶

^aNot measured or not available. ^bAbsorbance smaller than or very close to that of the blanks. ^cMAE is determined by normalizing b_{abs} to the organic aerosol (OA) mass measured by an Aerodyne AMS. ^dAn OA to OC mass ratio of 1.5 for coal-combustion influenced aerosols^{5,6} was applied. ^eValues obtained with the assumption that organic carbon is 100% soluble in methanol. ^fThe MAE values reported in various studies were estimated by normalizing b_{abs} to different proxies of organic mass, e.g., total OC, water-soluble OC (WSOC), water-insoluble OC (WIOC), methanol-soluble OC (MSOC), or OA by AMS. Note that the unit for MAE is $\text{m}^2 \text{g}^{-1}$ if normalizing b_{abs} to OA mass ($\mu\text{g m}^{-3}$) and is $\text{m}^2 \text{g}^{-1} \text{C}$ if normalizing to aerosol carbon mass ($\mu\text{g C m}^{-3}$).

$0.03 \text{ m}^2 \text{ g}^{-1}$) were very similar to that of aged OA, since SOA dominated the aged OA mass. Differences between $\text{MAE}_{\text{SOA},365}$ and $\text{MAE}_{\text{aged OA},365}$ were larger for coal B3, because POA also contributed significantly to the overall light absorption of BrC in the aged emissions, as shown in Figure 5b. The averaged $\text{MAE}_{\text{SOA},365}$ for coal B1 and B2 ($0.10 \pm 0.03 \text{ m}^2 \text{ g}^{-1}$) were slightly lower than that for coal B3 ($0.17 \pm 0.10 \text{ m}^2 \text{ g}^{-1}$). The $\text{MAE}_{\text{SOA},365}$ tended to decrease with increasing $\text{SOA}(t)/\text{OA}(t)$ (Figure 5d), relating the MAE_{SOA} to the SOA formation.

The $\text{MAE}_{\text{SOA},365}$ was two to nine times lower than the respective $\text{MAE}_{\text{POA},365}$ values for coal B1 and B2. For coal B3, the averaged $\text{MAE}_{\text{SOA},365}$ of aged OA#1 ($0.18 \pm 0.09 \text{ m}^2 \text{ g}^{-1}$) was one-eighth of the $\text{MAE}_{\text{POA},365}$. A further decrease in $\text{MAE}_{\text{SOA},365}$ of aged OA#2 was observed with increasing OH exposure. $\text{MAE}_{\text{SOA},365}$ decreases from $0.20 \pm 0.06 \text{ m}^2 \text{ g}^{-1}$ in aged OA#1 (OH exposure = $3.7 \times 10^7 \text{ molecules cm}^{-3} \text{ h}$) to $0.09 \pm 0.05 \text{ m}^2 \text{ g}^{-1}$ in aged OA#2 ($4.3 \times 10^7 \text{ molecules cm}^{-3} \text{ h}$) for experiment B3-10 and from $0.3 \pm 0.14 \text{ m}^2 \text{ g}^{-1}$ in aged OA#1 ($3.2 \times 10^7 \text{ molecules cm}^{-3} \text{ h}$) to $0.23 \pm 0.08 \text{ m}^2 \text{ g}^{-1}$ in aged OA#2 ($4.8 \times 10^7 \text{ molecules cm}^{-3} \text{ h}$) for B3-12. This may indicate either a real decrease in the mass-specific absorption of the SOA species with aging time or might be due to the assumption of constant MAE_{POA} in our calculations. If there is a decay (e.g., “bleaching”) in the MAE of pre-existing POA, this will decrease the $\text{MAE}_{\text{aged OA}}$. Since we assume constant MAE_{POA} in our calculations, the lower $\text{MAE}_{\text{aged OA}}$ will be attributed to a lower MAE_{SOA} .

3.4. Comparison with Previous Studies. In this study, we found that the MAE_{365} of methanol extracts from primary emissions ($0.84 \pm 0.54 \text{ m}^2 \text{ g}^{-1}$, with a range of $0.19\text{--}1.59 \text{ m}^2 \text{ g}^{-1}$) varied by coal types and was strongly affected by the combustion conditions. Table 1 summarizes the MAE_{365} of primary emissions from different coal, biomass, and vehicle types. The MAE values reported in various studies estimated by normalizing b_{abs} to different proxies of organic mass, such as total OC, WSOC, methanol-soluble OC (MSOC), or OA by AMS. Assuming an OA to OC mass ratio of 1.5:1 for coal-combustion influenced aerosols,⁶¹ the MAE_{365} of primary emissions in our study translates to $\sim 0.83 \text{ m}^2 \text{ g}^{-1} \text{ C}$ for coal B1, $\sim 0.81 \text{ m}^2 \text{ g}^{-1} \text{ C}$ for coal B2, and $\sim 2.2 \text{ m}^2 \text{ g}^{-1} \text{ C}$ for coal B3, with an average of $1.26 \text{ m}^2 \text{ g}^{-1} \text{ C}$. These values are consistent with those reported in the literature. For example, the methanol-extracted MAE_{365} of primary emissions from residential coal combustion was on average $1.51 \text{ m}^2 \text{ g}^{-1} \text{ C}$ by Yan et al.³⁵ and $0.9\text{--}2.8 \text{ m}^2 \text{ g}^{-1} \text{ C}$ by Li et al.,²⁵ similar in magnitude to the biomass burning emissions ($1.27 \pm 0.76 \text{ m}^2 \text{ g}^{-1} \text{ C}$ by Xie et al.¹⁶) but higher than that of gasoline vehicle emissions ($0.62 \pm 0.76 \text{ m}^2 \text{ g}^{-1} \text{ C}$ by Xie et al.¹⁶).

The MAE_{365} varies with extraction method (e.g., water or methanol) due to differences in the EE (eq 2). The MAE_{365} values of water extracts are always lower than those of methanol extracts, suggesting that chromophores dissolved in methanol have greater light absorption ability than those dissolved in water. For example, when light absorption spectra of both water and methanol extracts were measured, the MAE_{365} of methanol extracts was 1.5–2 times higher than that of coemitted WSOC for primary emissions of residential coal combustion.^{25,35,62} For water extracts, the MAE_{365} values for residential coal combustion ($1.10 \pm 0.16 \text{ m}^2 \text{ g}^{-1} \text{ C}$ by Yan et al.³⁵ and $0.3\text{--}1.0 \text{ m}^2 \text{ g}^{-1} \text{ C}$ by Li et al.²⁵) overlap with those for biomass burning and vehicular emissions.^{63,64}

As for SOA, the methanol-extracted MAE_{365} values estimated here for residential coal combustion for the first

time ($0.14 \text{ m}^2 \text{ g}^{-1}$ with a range of $0.05\text{--}0.30 \text{ m}^2 \text{ g}^{-1}$) were on average five times lower than those of POA. The MAE_{365} values for SOA obtained here fall into the range of those obtained from SOA from anthropogenic precursors, such as toluene and trimethylbenzene ($0.01\text{--}0.148 \text{ m}^2 \text{ g}^{-1}$),¹⁹ guaiacol, and naphthalene ($0.2\text{--}1.55 \text{ m}^2 \text{ g}^{-1}$),⁶⁵ but are approximately 1–2 orders of magnitude higher than the values reported for SOA from biogenic precursors such as isoprene and α -pinene.^{19,65}

In the aerosol phase, BrC light absorption is influenced by particle size and shape. Previous studies have predicted aerosol light absorption from MAE_{365} measurements using Mie models by assuming a spherical particle with specific mixing states. For example, on the basis of Mie calculations with the assumption that BrC and BC are externally mixed, Liu et al.⁵³ and Kumar et al.²³ suggested that the methanol-extracted MAE_{365} may be converted to that of particulate BrC by multiplication by a factor of about 1.8:

$$\text{MAC}_{365,\text{BrC}} = 1.8 \times \text{MAE}_{365} \quad (8)$$

where $\text{MAC}_{365,\text{BrC}}$ represents the mass absorption cross section of atmospheric BrC at 365 nm. Applying eq 8 to estimate the $\text{MAC}_{365,\text{BrC}}$ for primary coal combustion particles in this study gave $1.49 \text{ m}^2 \text{ g}^{-1} \text{ C}$ for coal B1, $1.46 \text{ m}^2 \text{ g}^{-1} \text{ C}$ for B2, and $3.87 \text{ m}^2 \text{ g}^{-1} \text{ C}$ for B3, with an average of $2.27 \text{ m}^2 \text{ g}^{-1} \text{ C}$. These values may be compared with the MAC of BC, $12 \pm 1 \text{ m}^2 \text{ g}^{-1}$ at 365 nm (calculated by extrapolating the value of $8.0 \pm 0.7 \text{ m}^2 \text{ g}^{-1}$ at 550 nm, recommended by Liu et al.⁶⁶ with an AAE_{BC} of 1). As expected, BrC from residential coal combustion absorbs less efficiently than BC at 365 nm. However, when considering that typical primary OC/BC mass ratios for emissions from bituminous coal range from 2 to 6,^{67,68} the light absorption by primary BrC can be comparable with BC at the shorter wavelength (365 nm). Taking into account the relatively low 450 nm SSA of the overall aerosol in this study, residential coal combustion could play an important role in the light absorption of BrC and should be considered in further modeling of OA radiative forcing.

■ ASSOCIATED CONTENT

Supporting Information

The Supporting Information is available free of charge at <https://pubs.acs.org/doi/10.1021/acs.est.0c08084>.

Discussions of coal, burner, and burning procedure, smog chamber, equivalent black carbon (eBC) measurement, UV–vis measurements, uncertainties of MAE, and sensitivity of $\text{POA}(t)$ on the $\text{SOA}(t)/\text{OA}(t)$ and MAE_{SOA} , figures of schematic of the smog chamber setup, eBC concentrations of primary and aged emissions, example solution spectra, absorption coefficient of blanks, MAE values, and proportion of SOA, and tables of coal properties by proximate and ultimate analysis, summary of filter samples from primary and aged emissions for UV–vis measurements, methanol-extracted MAE_{365} of primary and aged emissions, and averaged MAE_{365} of methanol extracts from residential coal combustion emissions (PDF)

■ AUTHOR INFORMATION

Corresponding Author

Ru-Jin Huang – State Key Laboratory of Loess and Quaternary Geology, Key Laboratory of Aerosol Chemistry

and Physics, CAS Center for Excellence in Quaternary Science and Global Change, Institute of Earth Environment, Chinese Academy of Sciences, Xi'an 710061, China; Institute of Global Environmental Change, Xi'an Jiaotong University, Xi'an 710049, China; orcid.org/0000-0002-4907-9616; Email: rujin.huang@ieecas.cn

Authors

Haiyan Ni – State Key Laboratory of Loess and Quaternary Geology, Key Laboratory of Aerosol Chemistry and Physics, CAS Center for Excellence in Quaternary Science and Global Change, Institute of Earth Environment, Chinese Academy of Sciences, Xi'an 710061, China; Centre for Isotope Research (CIO), Energy and Sustainability Research Institute Groningen (ESRIG), University of Groningen, 9747 AG Groningen, The Netherlands; orcid.org/0000-0001-5724-5867

Simone M. Pieber – Laboratory of Atmospheric Chemistry, Paul Scherrer Institute (PSI), Villigen 5232, Switzerland

Joel C. Corbin – Laboratory of Atmospheric Chemistry, Paul Scherrer Institute (PSI), Villigen 5232, Switzerland; orcid.org/0000-0002-2584-9137

Giulia Stefanelli – Laboratory of Atmospheric Chemistry, Paul Scherrer Institute (PSI), Villigen 5232, Switzerland

Veronika Pospisilova – Laboratory of Atmospheric Chemistry, Paul Scherrer Institute (PSI), Villigen 5232, Switzerland; orcid.org/0000-0003-2559-2252

Felix Klein – Laboratory of Atmospheric Chemistry, Paul Scherrer Institute (PSI), Villigen 5232, Switzerland

Martin Gysel-Beer – Laboratory of Atmospheric Chemistry, Paul Scherrer Institute (PSI), Villigen 5232, Switzerland

Lu Yang – State Key Laboratory of Loess and Quaternary Geology, Key Laboratory of Aerosol Chemistry and Physics, CAS Center for Excellence in Quaternary Science and Global Change, Institute of Earth Environment, Chinese Academy of Sciences, Xi'an 710061, China

Urs Baltensperger – Laboratory of Atmospheric Chemistry, Paul Scherrer Institute (PSI), Villigen 5232, Switzerland

Imad El Haddad – Laboratory of Atmospheric Chemistry, Paul Scherrer Institute (PSI), Villigen 5232, Switzerland; orcid.org/0000-0002-2461-7238

Jay G. Slowik – Laboratory of Atmospheric Chemistry, Paul Scherrer Institute (PSI), Villigen 5232, Switzerland

Junji Cao – State Key Laboratory of Loess and Quaternary Geology, Key Laboratory of Aerosol Chemistry and Physics, CAS Center for Excellence in Quaternary Science and Global Change, Institute of Earth Environment, Chinese Academy of Sciences, Xi'an 710061, China

André S. H. Prévôt – Laboratory of Atmospheric Chemistry, Paul Scherrer Institute (PSI), Villigen 5232, Switzerland; orcid.org/0000-0002-9243-8194

Ulrike Dusek – Centre for Isotope Research (CIO), Energy and Sustainability Research Institute Groningen (ESRIG), University of Groningen, 9747 AG Groningen, The Netherlands

Complete contact information is available at: <https://pubs.acs.org/10.1021/acs.est.0c08084>

Notes

The authors declare no competing financial interest.

ACKNOWLEDGMENTS

This work was supported by the National Natural Science Foundation of China (NSFC) under grant no. 41877408 and 41925015, and no. 91644219, the Chinese Academy of Sciences (no. ZDBS-LY-DQC001), the Cross Innovative Team fund from the State Key Laboratory of Loess and Quaternary Geology (SKLLQG) (no. SKLLQGT1801), the National Key Research and Development Program of China (no. 2017YFC0212701), and the grant KNAW (No. 530-5CDP30) from The Netherlands. A.S.H.P. received the financial support from the Sino-Swiss Science and Technology Cooperation (SSSTC) project HAZECHINA (no. IZLCZ2_169986). J.C.C. and M.G.-B. received financial support from the ERC under grant ERC-CoG-615922-BLACARAT.

REFERENCES

- (1) Chen, Y.; Bond, T. C. Light absorption by organic carbon from wood combustion. *Atmos. Chem. Phys.* **2010**, *10* (4), 1773–1787.
- (2) Kirchstetter, T. W.; Novakov, T.; Hobbs, P. V. Evidence that the spectral dependence of light absorption by aerosols is affected by organic carbon. *J. Geophys. Res.* **2004**, *109*, D21208.
- (3) Moschos, V.; Kumar, N. K.; Daellenbach, K. R.; Baltensperger, U.; Prévôt, A. S.; El Haddad, I. Source apportionment of brown carbon absorption by coupling UV/Vis spectroscopy with aerosol mass spectrometry. *Environ. Sci. Technol. Lett.* **2018**, *5* (6), 302–308.
- (4) Andreae, M.; Gelencsér, A. Black carbon or brown carbon? The nature of light-absorbing carbonaceous aerosols. *Atmos. Chem. Phys.* **2006**, *6* (10), 3131–3148.
- (5) Laskin, A.; Laskin, J.; Nizkorodov, S. A. Chemistry of atmospheric brown carbon. *Chem. Rev.* **2015**, *115* (10), 4335–4382.
- (6) Feng, Y.; Ramanathan, V.; Kotamarthi, V. Brown carbon: A significant atmospheric absorber of solar radiation? *Atmos. Chem. Phys.* **2013**, *13* (17), 8607–8621.
- (7) Lin, G.; Penner, J. E.; Flanner, M. G.; Sillman, S.; Xu, L.; Zhou, C. Radiative forcing of organic aerosol in the atmosphere and on snow: Effects of SOA and brown carbon. *J. Geophys. Res.: Atmos.* **2014**, *119* (12), 7453–7476.
- (8) Park, R. J.; Kim, M. J.; Jeong, J. I.; Youn, D.; Kim, S. A contribution of brown carbon aerosol to the aerosol light absorption and its radiative forcing in East Asia. *Atmos. Environ.* **2010**, *44* (11), 1414–1421.
- (9) Saleh, R.; Marks, M.; Heo, J.; Adams, P. J.; Donahue, N. M.; Robinson, A. L. Contribution of brown carbon and lensing to the direct radiative effect of carbonaceous aerosols from biomass and biofuel burning emissions. *J. Geophys. Res.: Atmos.* **2015**, *120* (19), 10285–10296.
- (10) Wang, X.; Heald, C.; Ridley, D.; Schwarz, J.; Spackman, J.; Perring, A.; Coe, H.; Liu, D.; Clarke, A. Exploiting simultaneous observational constraints on mass and absorption to estimate the global direct radiative forcing of black carbon and brown carbon. *Atmos. Chem. Phys.* **2014**, *14* (20), 10989–11010.
- (11) Wang, X.; Heald, C. L.; Sedlacek, A. J.; de Sá, S. S.; Martin, S. T.; Alexander, M. L.; Watson, T. B.; Aiken, A. C.; Springston, S. R.; Artaxo, P. Deriving brown carbon from multiwavelength absorption measurements: method and application to AERONET and Aethalometer observations. *Atmos. Chem. Phys.* **2016**, *16* (19), 12733–12752.
- (12) Bond, T. C. Spectral dependence of visible light absorption by carbonaceous particles emitted from coal combustion. *Geophys. Res. Lett.* **2001**, *28* (21), 4075–4078.
- (13) Chakrabarty, R. K.; Moosmüller, H.; Chen, L. W. A.; Lewis, K.; Arnott, W. P.; Mazzoleni, C.; Dubey, M. K.; Wold, C. E.; Hao, W. M.; Kreidenweis, S. M. Brown carbon in tar balls from smoldering biomass combustion. *Atmos. Chem. Phys.* **2010**, *10* (13), 6363–6370.
- (14) Lack, D. A.; Langridge, J. M.; Bahreini, R.; Cappa, C. D.; Middlebrook, A. M.; Schwarz, J. P. Brown carbon and internal mixing

in biomass burning particles. *Proc. Natl. Acad. Sci. U. S. A.* **2012**, *109*, 14802–14807.

(15) Shetty, N. J.; Pandey, A.; Baker, S.; Hao, W. M.; Chakrabarty, R. K. Measuring light absorption by freshly emitted organic aerosols: optical artifacts in traditional solvent-extraction-based methods. *Atmos. Chem. Phys.* **2019**, *19* (13), 8817–8830.

(16) Xie, M.; Hays, M.; Holder, A. Light-absorbing organic carbon from prescribed and laboratory biomass burning and gasoline vehicle emissions. *Sci. Rep.* **2017**, *7* (1), 7318.

(17) Lu, Z.; Streets, D. G.; Winijkul, E.; Yan, F.; Chen, Y.; Bond, T. C.; Feng, Y.; Dubey, M. K.; Liu, S.; Pinto, J. P.; et al. Light Absorption properties and radiative effects of primary organic aerosol emissions. *Environ. Sci. Technol.* **2015**, *49* (8), 4868–4877.

(18) Saleh, R.; Robinson, E. S.; Tkacik, D. S.; Ahern, A. T.; Liu, S.; Aiken, A. C.; Sullivan, R. C.; Presto, A. A.; Dubey, M. K.; Yokelson, R. J.; Donahue, N. M.; Robinson, A. L. Brownness of organics in aerosols from biomass burning linked to their black carbon content. *Nat. Geosci.* **2014**, *7* (9), 647–650.

(19) Liu, J.; Lin, P.; Laskin, A.; Laskin, J.; Kathmann, S. M.; Wise, M.; Caylor, R.; Imholt, F.; Selimovic, V.; Shilling, J. E. Optical properties and aging of light-absorbing secondary organic aerosol. *Atmos. Chem. Phys.* **2016**, *16* (19), 12815–12827.

(20) Zhao, R.; Lee, A.; Huang, L.; Li, X.; Yang, F.; Abbatt, J. Photochemical processing of aqueous atmospheric brown carbon. *Atmos. Chem. Phys.* **2015**, *15* (11), 6087–6100.

(21) Dasari, S.; Andersson, A.; Bikkina, S.; Holmstrand, H.; Budhavant, K.; Sathesh, S.; Asmi, E.; Kesti, J.; Backman, J.; Salam, A.; Bisht, D. S.; Tiwari, S.; Hameed, Z.; Gustafsson, Ö. Photochemical degradation affects the light absorption of water-soluble brown carbon in the South Asian outflow. *Sci. Adv.* **2019**, *5* (1), No. eaau8066.

(22) Lee, H. J.; Aiona, P. K.; Laskin, A.; Laskin, J.; Nizkorodov, S. A. Effect of solar radiation on the optical properties and molecular composition of laboratory proxies of atmospheric brown carbon. *Environ. Sci. Technol.* **2014**, *48* (17), 10217–10226.

(23) Kumar, N. K.; Corbin, J. C.; Bruns, E. A.; Massabó, D.; Slowik, J. G.; Drinovec, L.; Močnik, G.; Prati, P.; Vlachou, A.; Baltensperger, U.; Gysel, M.; El-Haddad, I.; Prévôt, A. S. H. Production of particulate brown carbon during atmospheric aging of residential wood-burning emissions. *Atmos. Chem. Phys.* **2018**, *18* (24), 17843–17861.

(24) Zhong, M.; Jang, M. Dynamic light absorption of biomass-burning organic carbon photochemically aged under natural sunlight. *Atmos. Chem. Phys.* **2014**, *14* (3), 1517–1525.

(25) Li, M.; Fan, X.; Zhu, M.; Zou, C.; Song, J.; Wei, S.; Jia, W.; Peng, P. a. Abundance and light absorption properties of brown carbon emitted from residential coal combustion in China. *Environ. Sci. Technol.* **2019**, *53* (2), 595–603.

(26) Sun, J.; Zhi, G.; Hitznerberger, R.; Chen, Y.; Tian, C.; Zhang, Y.; Feng, Y.; Cheng, M.; Zhang, Y.; Cai, J.; Chen, F.; Qiu, Y.; Jiang, Z.; Li, J.; Zhang, G.; Mo, Y. Emission factors and light absorption properties of brown carbon from household coal combustion in China. *Atmos. Chem. Phys.* **2017**, *17* (7), 4769–4780.

(27) Tian, J.; Wang, Q.; Ni, H.; Wang, M.; Zhou, Y.; Han, Y.; Shen, Z.; Pongpiachan, S.; Zhang, N.; Zhao, Z.; Zhang, Q.; Zhang, Y.; Long, X.; Cao, J. Emission characteristics of primary brown carbon absorption from biomass and coal burning: development of an optical emission inventory for China. *J. Geophys. Res.: Atmos.* **2019**, *124* (3), 1879–1893.

(28) Elser, M.; Huang, R.-J.; Wolf, R.; Slowik, J. G.; Wang, Q.; Canonaco, F.; Li, G.; Bozzetti, C.; Daellenbach, K. R.; Huang, Y.; et al. New insights into PM_{2.5} chemical composition and sources in two major cities in China during extreme haze events using aerosol mass spectrometry. *Atmos. Chem. Phys.* **2016**, *16* (5), 3207–3225.

(29) Huang, R.-J.; Zhang, Y.; Bozzetti, C.; Ho, K.-F.; Cao, J.-J.; Han, Y.; Daellenbach, K. R.; Slowik, J. G.; Platt, S. M.; Canonaco, F.; Zotter, P.; Wolf, R.; Pieber, S. M.; Bruns, E. A.; Crippa, M.; Ciarelli, G.; Piazzalunga, A.; Schwikowski, M.; Abbaszade, G.; Schnelle-Kreis, J.; Zimmermann, R.; An, Z.; Szidat, S.; Baltensperger, U.; Haddad, I. E.; Prévôt, A. S. H. High secondary aerosol contribution to particulate

pollution during haze events in China. *Nature* **2014**, *514* (7521), 218–222.

(30) Kalaiarasan, G.; Balakrishnan, R. M.; Khaparde, V. Receptor model based source apportionment of PM₁₀ in the metropolitan and industrialized areas of Mangalore. *Environ. Technol. Inno.* **2016**, *6*, 195–203.

(31) Junninen, H.; Mønster, J.; Rey, M.; Cancelinha, J.; Douglas, K.; Duane, M.; Forcina, V.; Müller, A.; Lagler, F.; Marelli, L.; et al. Quantifying the impact of residential heating on the urban air quality in a typical European coal combustion region. *Environ. Sci. Technol.* **2009**, *43* (20), 7964–7970.

(32) Lin, C.; Ceburnis, D.; Hellebust, S. M.; Buckley, P.; Wenger, J. C.; Canonaco, F.; Prevot, A. S. H.; Huang, R.-J.; O'Dowd, C.; O'vadnevaite, J. Characterization of primary organic aerosol from domestic wood, peat, and coal burning in Ireland. *Environ. Sci. Technol.* **2017**, *51* (18), 10624–10632.

(33) National Bureau of Statistics and National Energy Administration. *China Energy Statistical Yearbook*; China Statistics Press: Beijing, China, 2016.

(34) Xie, C.; Xu, W.; Wang, J.; Wang, Q.; Liu, D.; Tang, G.; Chen, P.; Du, W.; Zhao, J.; Zhang, Y.; Zhou, W.; Han, T.; Bian, Q.; Li, J.; Fu, P.; Wang, Z.; Ge, X.; Allan, J.; Coe, H.; Sun, Y. Vertical characterization of aerosol optical properties and brown carbon in winter in urban Beijing, China. *Atmos. Chem. Phys.* **2019**, *19* (1), 165–179.

(35) Yan, C.; Zheng, M.; Bosch, C.; Andersson, A.; Desyaterik, Y.; Sullivan, A. P.; Collett, J. L.; Zhao, B.; Wang, S.; He, K.; et al. Important fossil source contribution to brown carbon in Beijing during winter. *Sci. Rep.* **2017**, *7* (1), 43182.

(36) Bertrand, A.; Stefenelli, G.; Bruns, E. A.; Pieber, S. M.; Temime-Roussel, B.; Slowik, J. G.; Prévôt, A. S. H.; Wortham, H.; El Haddad, I.; Marchand, N. Primary emissions and secondary aerosol production potential from woodstoves for residential heating: Influence of the stove technology and combustion efficiency. *Atmos. Environ.* **2017**, *169*, 65–79.

(37) Bruns, E. A.; El Haddad, I.; Slowik, J. G.; Kilic, D.; Klein, F.; Baltensperger, U.; Prévôt, A. S. Identification of significant precursor gases of secondary organic aerosols from residential wood combustion. *Sci. Rep.* **2016**, *6* (1), 27881.

(38) Platt, S. M.; El Haddad, I.; Pieber, S. M.; Zardini, A. A.; Suarez-Bertoa, R.; Clairotte, M.; Daellenbach, K. R.; Huang, R. J.; Slowik, J. G.; Hellebust, S.; Temime-Roussel, B.; Marchand, N.; de Gouw, J.; Jimenez, J. L.; Hayes, P. L.; Robinson, A. L.; Baltensperger, U.; Astorga, C.; Prévôt, A. S. H. Gasoline cars produce more carbonaceous particulate matter than modern filter-equipped diesel cars. *Sci. Rep.* **2017**, *7* (1), 4926.

(39) Taira, M.; Kanda, Y. Continuous generation system for low-concentration gaseous nitrous acid. *Anal. Chem.* **1990**, *62* (6), 630–633.

(40) Barmet, P.; Dommen, J.; DeCarlo, P.; Tritscher, T.; Praplan, A.; Platt, S.; Prévôt, A.; Donahue, N.; Baltensperger, U. OH clock determination by proton transfer reaction mass spectrometry at an environmental chamber. *Atmos. Meas. Tech.* **2012**, *5* (3), 647–656.

(41) Klein, F.; Pieber, S. M.; Ni, H.; Stefenelli, G.; Bertrand, A.; Kilic, D.; Pospisilova, V.; Temime-Roussel, B.; Marchand, N.; El Haddad, I.; et al. Characterization of gas-phase organics using proton transfer reaction time-of-flight mass spectrometry: Residential coal combustion. *Environ. Sci. Technol.* **2018**, *52* (5), 2612–2617.

(42) Williams, L. R.; Gonzalez, L. A.; Peck, J.; Trimborn, D.; McInnis, J.; Farrar, M. R.; Moore, K. D.; Jayne, J. T.; Robinson, W. A.; Lewis, D. K.; Onasch, T. B.; Canagaratna, M. R.; Trimborn, A.; Timko, M. T.; Magoon, G.; Deng, R.; Tang, D.; de la Rosa Blanco, E.; Prévôt, A. S. H.; Smith, K. A.; Worsnop, D. R. Characterization of an aerodynamic lens for transmitting particles greater than 1 micrometer in diameter into the Aerodyne aerosol mass spectrometer. *Atmos. Meas. Tech.* **2013**, *6* (11), 3271–3280.

(43) Pieber, S. M.; El Haddad, I.; Slowik, J. G.; Canagaratna, M. R.; Jayne, J. T.; Platt, S. M.; Bozzetti, C.; Daellenbach, K. R.; Fröhlich, R.; Vlachou, A.; et al. Inorganic salt interference on CO₂⁺ in aerodyne

AMS and ACSM organic aerosol composition studies. *Environ. Sci. Technol.* **2016**, *50* (19), 10494–10503.

(44) Drinovec, L.; Močnik, G.; Zotter, P.; Prévôt, A.; Ruckstuhl, C.; Coz, E.; Rupakheti, M.; Sciare, J.; Müller, T.; Wiedensohler, A.; et al. The "dual-spot" Aethalometer: An improved measurement of aerosol black carbon with real-time loading compensation. *Atmos. Meas. Tech.* **2015**, *8* (5), 1965–1979.

(45) Platt, S. M.; El Haddad, I.; Zardini, A. A.; Clairotte, M.; Astorga, C.; Wolf, R.; Slowik, J. G.; Temime-Roussel, B.; Marchand, N.; Ježek, I.; Drinovec, L.; Močnik, G.; Möhler, O.; Richter, R.; Barmet, P.; Bianchi, F.; Baltensperger, U.; Prévôt, A. S. H. Secondary organic aerosol formation from gasoline vehicle emissions in a new mobile environmental reaction chamber. *Atmos. Chem. Phys.* **2013**, *13* (18), 9141–9158.

(46) Grieshop, A.; Donahue, N.; Robinson, A. Laboratory investigation of photochemical oxidation of organic aerosol from wood fires 2: analysis of aerosol mass spectrometer data. *Atmos. Chem. Phys.* **2009**, *9* (6), 2227–2240.

(47) Krapf, M.; El Haddad, I.; Bruns, E. A.; Molteni, U.; Daellenbach, K. R.; Prevot, A. S. H.; Baltensperger, U.; Dommen, J. Labile peroxides in secondary organic aerosol. *Chem.* **2016**, *1* (4), 603–616.

(48) Cheng, Y.; He, K.-b.; Du, Z.-y.; Engling, G.; Liu, J.-m.; Ma, Y.-l.; Zheng, M.; Weber, R. J. The characteristics of brown carbon aerosol during winter in Beijing. *Atmos. Environ.* **2016**, *127*, 355–364.

(49) Schnitzler, E. G.; Liu, T.; Hems, R. F.; Abbatt, J. P. D. Emerging investigator series: heterogeneous OH oxidation of primary brown carbon aerosol: effects of relative humidity and volatility. *Environ. Sci.: Processes Impacts* **2020**, *22* (11), 2162–2171.

(50) Zhou, J.; Elser, M.; Huang, R. J.; Krapf, M.; Fröhlich, R.; Bhattu, D.; Stefanelli, G.; Zotter, P.; Bruns, E. A.; Pieber, S. M.; Ni, H.; Wang, Q.; Wang, Y.; Zhou, Y.; Chen, C.; Xiao, M.; Slowik, J. G.; Brown, S.; Cassagnes, L. E.; Daellenbach, K. R.; Nussbaumer, T.; Geiser, M.; Prévôt, A. S. H.; El-Haddad, I.; Cao, J.; Baltensperger, U.; Dommen, J. Predominance of secondary organic aerosol to particle-bound reactive oxygen species activity in fine ambient aerosol. *Atmos. Chem. Phys.* **2019**, *19* (23), 14703–14720.

(51) Hecobian, A.; Zhang, X.; Zheng, M.; Frank, N.; Edgerton, E. S.; Weber, R. J. Water-soluble organic aerosol material and the light-absorption characteristics of aqueous extracts measured over the Southeastern United States. *Atmos. Chem. Phys.* **2010**, *10* (13), 5965–5977.

(52) Huang, R.-J.; Yang, L.; Cao, J.; Chen, Y.; Chen, Q.; Li, Y.; Duan, J.; Zhu, C.; Dai, W.; Wang, K.; Lin, C.; Ni, H.; Corbin, J. C.; Wu, Y.; Zhang, R.; Tie, X.; Hoffmann, T.; O'Dowd, C.; Dusek, U. Brown carbon aerosol in urban Xi'an, northwest China: The composition and light absorption properties. *Environ. Sci. Technol.* **2018**, *52* (12), 6825–6833.

(53) Liu, J.; Bergin, M.; Guo, H.; King, L.; Kotra, N.; Edgerton, E.; Weber, R. J. Size-resolved measurements of brown carbon in water and methanol extracts and estimates of their contribution to ambient fine-particle light absorption. *Atmos. Chem. Phys.* **2013**, *13* (24), 12389–12404.

(54) Zhang, X.; Lin, Y.-H.; Surratt, J. D.; Weber, R. J. Sources, composition and absorption Ångström exponent of light-absorbing organic components in aerosol extracts from the Los Angeles Basin. *Environ. Sci. Technol.* **2013**, *47* (8), 3685–3693.

(55) Hays, M. D.; Fine, P. M.; Geron, C. D.; Kleeman, M. J.; Gullett, B. K. Open burning of agricultural biomass: Physical and chemical properties of particle-phase emissions. *Atmos. Environ.* **2005**, *39* (36), 6747–6764.

(56) McMeeking, G. R.; Kreidenweis, S. M.; Baker, S.; Carrico, C. M.; Chow, J. C.; Collett, J. L.; Hao, W. M.; Holden, A. S.; Kirchstetter, T. W.; Malm, W. C.; Moosmüller, H.; Sullivan, A. P.; Wold, C. E. Emissions of trace gases and aerosols during the open combustion of biomass in the laboratory. *J. Geophys. Res.* **2009**, *114* (D19), D19210.

(57) Li, X.; Chen, Y.; Bond, T. C. Light absorption of organic aerosol from pyrolysis of corn stalk. *Atmos. Environ.* **2016**, *144*, 249–256.

(58) Forrister, H.; Liu, J.; Scheuer, E.; Dibb, J.; Ziemba, L.; Thornhill, K. L.; Anderson, B.; Diskin, G.; Perring, A. E.; Schwarz, J. P.; Campuzano-Jost, P.; Day, D. A.; Palm, B. B.; Jimenez, J. L.; Nenes, A.; Weber, R. J. Evolution of brown carbon in wildfire plumes. *Geophys. Res. Lett.* **2015**, *42*, 4623–4630.

(59) Haywood, J. M.; Shine, K. P. The effect of anthropogenic sulfate and soot aerosol on the clear sky planetary radiation budget. *Geophys. Res. Lett.* **1995**, *22* (5), 603–606.

(60) Bond, T. C.; Bergstrom, R. W. Light absorption by carbonaceous particles: An investigative review. *Aerosol Sci. Technol.* **2006**, *40* (1), 27–67.

(61) Xing, L.; Fu, T.-M.; Cao, J.; Lee, S.; Wang, G.; Ho, K.; Cheng, M.-C.; You, C.-F.; Wang, T. Seasonal and spatial variability of the OM/OC mass ratios and high regional correlation between oxalic acid and zinc in Chinese urban organic aerosols. *Atmos. Chem. Phys.* **2013**, *13* (8), 4307–4318.

(62) Wang, Y.; Song, S.; Wang, T.; Li, D.; Tan, H. Effects of coal types and combustion conditions on carbonaceous aerosols in flue gas and their light absorption properties. *Fuel* **2020**, *277*, 118148.

(63) Du, Z.; He, K.; Cheng, Y.; Duan, F.; Ma, Y.; Liu, J.; Zhang, X.; Zheng, M.; Weber, R. A yearlong study of water-soluble organic carbon in Beijing II: Light absorption properties. *Atmos. Environ.* **2014**, *89*, 235–241.

(64) Hu, Z.; Kang, S.; Li, C.; Yan, F.; Chen, P.; Gao, S.; Wang, Z.; Zhang, Y.; Sillanpää, M. Light absorption of biomass burning and vehicle emission-sourced carbonaceous aerosols of the Tibetan Plateau. *Environ. Sci. Pollut. Res.* **2017**, *24* (18), 15369–15378.

(65) Romonosky, D. E.; Ali, N. N.; Saiduddin, M. N.; Wu, M.; Lee, H. J.; Aiona, P. K.; Nizkorodov, S. A. Effective absorption cross sections and photolysis rates of anthropogenic and biogenic secondary organic aerosols. *Atmos. Environ.* **2016**, *130*, 172–179.

(66) Liu, F.; Yon, J.; Fuentes, A.; Lobo, P.; Smallwood, G. J.; Corbin, J. C. Review of recent literature on the light absorption properties of black carbon: refractive index, mass absorption cross section, and absorption function. *Aerosol Sci. Technol.* **2020**, *54* (1), 33–51.

(67) Chen, Y. J.; Tian, C. G.; Feng, Y. L.; Zhi, G. R.; Li, J.; Zhang, G. Measurements of emission factors of PM_{2.5}, OC, EC, and BC for household stoves of coal combustion in China. *Atmos. Environ.* **2015**, *109*, 190–196.

(68) Zhi, G.; Chen, Y.; Feng, Y.; Xiong, S.; Li, J.; Zhang, G.; Sheng, G.; Fu, J. Emission characteristics of carbonaceous particles from various residential coal-stoves in China. *Environ. Sci. Technol.* **2008**, *42* (9), 3310–3315.